ACS Macro Letters

Letter

pubs.acs.org/macroletters

A Universal Scaling Analysis of Nonisothermal Kinetics in Block Copolymer Phase Transitions

Julian D. Spring and Rama Bansil*

Department of Physics, Boston University, Boston, Massachusetts 02215, United States

Supporting Information

ABSTRACT: Recently, Farjas and Roura (FR) have proposed a universal scaling law to describe *nonisothermal* crystallization kinetics based on a modification of the conventionally used Avrami model. In this letter, we apply the approach of Farjas and Roura to analyze the kinetics of an order−order phase transition in a diblock copolymer solution. We present an analysis of kinetics of the hexagonally packed cylinders (HEX) to gyroid transformation in polystyrene-*b*-polyisoprene (SI) diblock copolymer solutions in dimethyl phthalate using time-resolved small-angle X-ray scattering (SAXS) measurements. By shifting and scaling time in terms of the time at which the transformation rate is maximal, data for samples at two different concentrations at different ramp rates collapse onto the single universal curve predicted by Farjas and Roura. The activation energy for this process was estimated by fitting to the FR model. An estimate of the activation energy was also obtained by Avrami analysis of temperature jump experiments on the same sample. These two estimates differ by a factor of 2, suggesting that the two methods probe different stages of the phase transformation.

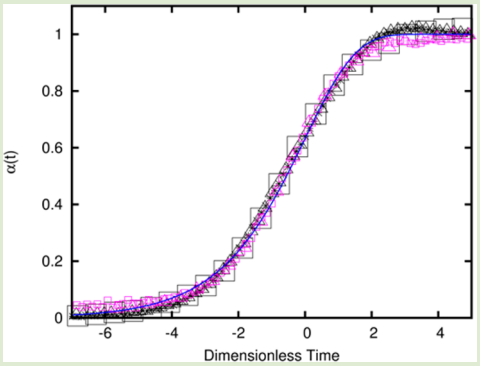

The Avrami equation, also known as the Johnson−Mehl−Avrami−Kolmogorov (JMAK) equation, has been extensively used to study the kinetics of phase transitions.[1−5] For example, Google Scholar shows over 2000 citations to the 1939 Avrami paper[1−3] with the keyword polymer and over 200 for block copolymers. The JMAK theory is derived for growth of the transformed phase under isothermal conditions, and the kinetic growth rate depends on the depth of the jump below the equilibrium phase transition temperature. Isothermal conditions are nontrivial to meet experimentally, as even in the best designed rapid temperature jump (T-jump) experiments there is always a finite time required to change temperature, so the phase transition already initiates while the system's temperature is reaching its final value. Thus, the validity of the JMAK analysis is justified when the induction period is long compared to the temperature equilibration time. While this may hold for polymer melts, it is not a good approximation for block copolymer solution transitions where the phase transformation is faster and induction time smaller than the sample's temperature equilibration time. An alternative to T-jump measurements that is much easier to implement experimentally is to follow the transformation by ramping the temperature at a controlled rate through the phase transition. Temperature ramp (T-ramp) experiments are routinely used to determine the phase transition temperature, but there are few nonisothermal kinetic theories[6,7] which have been applied primarily to polymer crystallization. Moreover, the interpretation of these theories is often not straightforward.[8,9]

Recently Farjas and Roura (FR)[10,11] have proposed a modification to the JMAK equation specifically applicable to the cases of monotonic heating and cooling. They obtained a universal scaling law which allows analysis akin to the JMAK analysis, with the time scaled according to kinetic parameters. Their method has been successfully applied to amorphous silicon.[11] To the best of our knowledge, this approach has not been applied to order−disorder and order−order transitions (OOT) in block copolymers. In this letter, we apply the FR model to analyze the kinetics of the hexagonally packed cylinders (HEX) to gyroid transformation in a polystyrene-*b*-polyisoprene (SI) diblock copolymer and show that data at different heating rates collapse onto a universal scaling function. The HEX to gyroid transition has been studied extensively, both theoretically[12,13] and experimentally,[14−16] and has been shown to proceed epitaxially, with the first-order Bragg peak of the HEX phase transforming smoothly into the first-order gyroid peak.

Time-resolved small-angle X-ray scattering (SAXS) from SI(16−11) diblock was used to probe both the physical structure of the ordered phase as well as the transformation kinetics following either a T-jump or T-ramp. Concentrations of 75% and 80% w/v in dimethyl phthalate (DMP) were investigated. These polymer solutions have an order−order transition temperature (T_{OOT}) from HEX to gyroid near 117 and 106 °C for the 75% and 80% w/v solutions, respectively. Lodge et al.[15] reported a phase diagram for a similar diblock, SI(15−13), which shows T_{OOT} values comparable to these at concentrations of 60% and 70% w/v in DMP.

Received: April 8, 2013
Accepted: July 23, 2013
Published: July 29, 2013

   dx.doi.org/10.1021/mz400172x | *ACS Macro Lett.* 2013, 2, 745−748

Figure 1 shows the time evolution of the SAXS profiles, $I(q,T)$ vs q as a function of temperature during a T-ramp where the

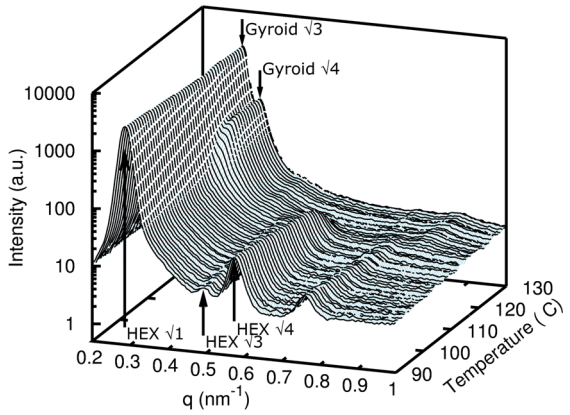

Figure 1. Time evolution of SAXS intensity $I(q)$ vs q during a T-ramp from 90 to 130 °C at 0.5 °C/min. Note the light bands on the slope of the primary peak, indicating intensity growth at constant q.

temperature is increased at a constant rate β = 0.5 °C/min. A clear transition from HEX to gyroid is visible at 117 °C. The primary peak of the HEX phase transitions epitaxially into the primary $(\sqrt{3})$ gyroid peak, with a small shift in the peak position toward higher q, in agreement with previous observations.[12−16] The light bands on the steep part of the primary scattering peak follow lines of constant q, indicating the growth of the gyroid $\sqrt{4}$ peak. In view of this epitaxial transformation the first peak intensity cannot be used to determine the fraction of transformed material. To get an accurate measure of the transformed fraction of material, we follow the approach of Floudas et al.,[14] determining the fraction of transformed material from the measured scattered intensity, $I_2(q_2)$, at the expected position of the second-order gyroid peak ($q_2 = (4/3)^{1/2}q^*$, where q^* is the position of the first-order peak) as a function of temperature and time.

As mentioned above, the JMAK equation describes the time evolution with the well-known stretched exponential form

$$a(t) = 1 - \exp[-(kt)^n] \tag{1}$$

where α is the fraction of transformed material; k is the rate constant; t is time; and n is the Avrami exponent describing the growth of the new phase. The rate constant k depends on the final temperature T, the depth of the T-jump, the activation energy; and the nucleation rate. As a consequence, eq 1 is applicable in situations where temperature can be equilibrated rapidly enough into the new phase regime such that T can be considered to be constant during the evolution of the new phase.

In the case of isothermal kinetics assuming constant nucleation, $n = m + 1$, and the argument of the exponent has the value $(kt)^{m+1}$. In general this quantity is the extended transformed fraction α_{ex}, which is the equivalent fraction of transformed material if expanding nuclei could grow through each other without mutual interference.[1] This extended fraction depends on the time-integrated nucleation and growth rates of the new phase, but these rates depend on temperature, which produces time dependence in the nonisothermal case and makes the search for a solution a nontrivial endeavor. Farjas and Roura[10,11] use a time scaling constant related to the nucleation and growth rates to arrive at a universal solution that does not depend on these rates, thus eliminating T-dependence and producing the final scaled solution in terms of a dimensionless time t'. The universal scaled form for the fraction of transformed material $\alpha(t')$ is written as

$$a(t') = 1 - \exp[-(\exp[\kappa C t'])^{m+1}] \tag{2}$$

The parameters C and κ are related to the activation energy and the Avrami exponent by

$$C \equiv \left[\frac{(m+1)!E^{m+1}}{\prod_{i=0}^{m}(E_N + iE_G)}\right]^{1/(m+1)} \tag{3}$$

$$\kappa \equiv \sqrt[m+1]{\frac{\sigma}{m+1}} \tag{4}$$

where

$$E = \frac{E_N + mE_G}{m+1} \tag{5}$$

Here E_N and E_G are the nucleation and growth activation energies, respectively, and κ is defined by a shape factor σ, which depends on the geometry of the growth of the new phase.[11]

For a linear ramp, temperature increases linearly with measured time (t_m), i.e., $T = T_0 + \beta t_m$, where T_0 is the initial temperature at $t_m = 0$ and β is the constant rate at which temperature changes. The dimensionless time t' in eq 2 is obtained by scaling and shifting real time such that the origin of dimensionless time is shifted to correspond to t_p, corresponding to the temperature T_p at which the growth of the fraction of transformed material is maximal, i.e.

$$\left.\frac{d^2\alpha}{dt^2}\right|_{T_p} = 0 \tag{6}$$

The time scale is set in terms of the maximal growth rate, $\kappa C/\tau_p$, where

$$\tau_p \equiv (IG^m)^{-1/(m+1)}|_{T=T_p} = (I_0G_0)^{-1/(m+1)}\left(\exp\left[\frac{E}{k_BT_p}\right]\right) \tag{7}$$

Thus $t' = (t_m - t_p)/\tau_p = (T - T_p)/(\beta\tau_p)$. The nucleation and growth rates I and G are assumed to be of the Arrhenius form in the definition of τ_p.

Figure 2 shows the time evolution of the second peak intensity $I_2(q_2)$ for three different ramp rates. The data show a clear sigmoidal curve for all three ramp rates, with the onset of the HEX → gyroid transition occurring earlier for faster rates. The measured T_{OOT}, characterized by the peak temperature T_p, depends on the ramp rate, decreasing from 119.4 to 119.0 °C as the ramp rate decreases from 1.0 to 0.3 °C/min.

We use the gyroid peak intensity I_2 to estimate the fraction of transformed material, which varies from zero to unity. By subtracting the baseline offset and normalizing by the maximum value of I_2, we convert $I_2(t)$ to $\alpha(t)$. After the time origin is set by T_p, eq 2 can be fitted by a single rate parameter $A = \kappa C/\tau_p$. The values of the rate parameters A were 0.329, 0.125, and 0.079 min^{-1} for 1.0, 0.5, and 0.3 °C/min ramp rates, respectively. These values indicate that the transformation happens faster for higher ramp rates and is not simply scaled by the ramp rate factors β.

dx.doi.org/10.1021/mz400172x | ACS Macro Lett. 2013, 2, 745−748

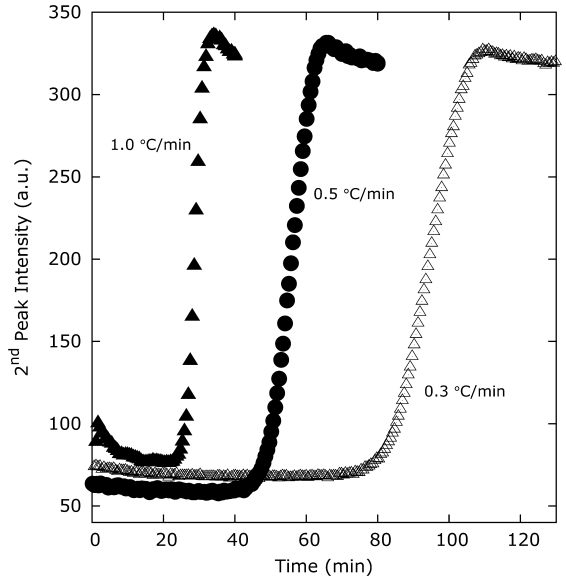

Figure 2. Time evolution of the second-order gyroid peak intensity for ramp rates of 1.0, 0.5, and 0.3 °C/min.

To test the validity of this scaling approach for our data we used the 1 °C/min ramp data (A_1) as our reference. We can scale the time for another ramp rate accordingly by using the ratio A_2/A_1. As shown in Figure 3, the growth curves for these

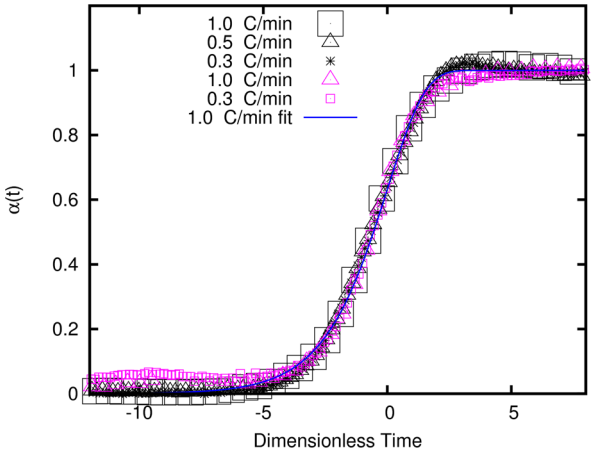

Figure 3. Time evolution of the fraction of transformed material, $\alpha(t)$ for two SI in DMP samples (75% in black, 80% in magenta) at three different ramp rates. The time has been shifted and scaled to the same dimensionless time, t', as described in the text.

three ramp rates collapse onto a single master curve, confirming a universal scaling law. The collapsed data are also well-fitted by eq 2, demonstrating the suitability of the FR approach to study block copolymer order−order phase transitions. In addition to data from three different ramp rates of the SI 75% sample, we have also plotted in Figure 3 data for two ramps from a different sample at SI 80% which also collapse onto the same curve with A = 0.287 for 1 °C/min and A = 0.092 for 0.3 °C/min. Another data set, using SI 75% at 1 °C/min from a previous run (data not shown) also collapses on to the same universal curve, further confirming the validity of this scaled equation.

It is worth noting that the sigmoidal order−order growth curves could be fit using other sigmoidal functions, such as a simple hyperbolic tangent as well as the Ozawa theory of nonisothermal growth kinetics. Figure S1 (Supporting Information) shows a comparison of the Ozawa and tanh functions to the FR model, fitted to the same T-ramp data. The FR fit appears to be the best overall, fitting to a root-mean-square (RMS) deviation of 1.5% per data point; the tanh function captures the initial time evolution better but systematically deviates at late times. The Ozawa model[6] gives the fraction of transformed material $\alpha(T)$ for a heating rate β as

$$\alpha(T) = 1 - \exp\left[-k_0\beta^{-n}\exp\left\{-\frac{1.0518mE}{RT}\right\}\right] \quad (8)$$

This equation is the least well-fit, with an RMS deviation twice as large as that of the FR fit. Moreover, the two parameters (pre-exponential rate constant k_0 and activation energy E) are strongly correlated, with a correlation coefficient of 0.997, as opposed to 0.28 for the two parameters A and T_P in the FR analysis. While the function $\alpha(t) = A\tanh(t/\tau)$ could in principle be scaled, it provides no physical insight into the characteristic time τ. The Ozawa equation depends in a complex way on $1/T$, excluding the possibility of using the approach of shifting and scaling the temperature to collapse the data for different ramps in any meaningful way. A similar reason for lack of scaling also applies to the Kissinger model.[7]

Assuming that the transformation takes place over a narrow range of temperature, FR relates the fitted rate parameter A to the activation energy E by[11]

$$E = \frac{k_B A T_P^2}{\beta} \quad (9)$$

Using eq 9, we obtain E = 350 ± 10 kJ/mol for the 80% sample and E = 360 ± 60 kJ/mol for the 75% sample.

Activation energies can also be obtained by Avrami analysis of T-jump data.[14] The higher T_{OOT} of the 75% samples makes it difficult to get reliable T-jump data due to experimental limitations of the temperature controller. In view of this, the results of Avrami analysis on T-jump data for SI 80% will be compared to those obtained from the FR analysis for the same sample. Figure 4a shows the time evolution of the SAXS profiles following a T-jump from 80° to 110 °C for the SI 80% sample. The transformation of HEX to gyroid is completed in approximately 45 min. The peak intensity of the second peak was used to determine the fraction of transformed material, $\alpha(t)$. The JMAK equation (eq 1) can be transformed into a linear form by defining $f(\alpha) = \ln[-\ln(1-\alpha)] = K + n(\ln[t])$, where $K = n(\ln[k])$. Figure 4b, a plot of $f(\alpha)$ vs $\ln[t]$, shows two stages in the growth of the gyroid phase, in agreement with the earlier results of Floudas et al.[14] The first stage which occurs partly during the temperature equilibration time and also reflects the initial structural rearrangement of the HEX morphology does not fit the JMAK equation, while the second stage can be fitted to the JMAK equation with n = 1.5. Fitting of the second stage data for two different T-jumps to the JMAK equation enabled us to obtain an estimate of the activation energy using $E = (k_B \ln(k_1/k_2))/(1/T_2 - 1/T_1)$. This procedure gives E = 190 ± 30 kJ/mol for the 80% w/v sample. The actual statistical error based on more measurements is likely to be greater than that based on the fitting accuracy. Nevertheless, the discrepancy in activation energies obtained by the FR analysis of T-ramp and JMAK analysis of T-jump data is too large to be only due to statistical and experimental errors. A possible explanation for this difference is

dx.doi.org/10.1021/mz400172x | ACS Macro Lett. 2013, 2, 745−748

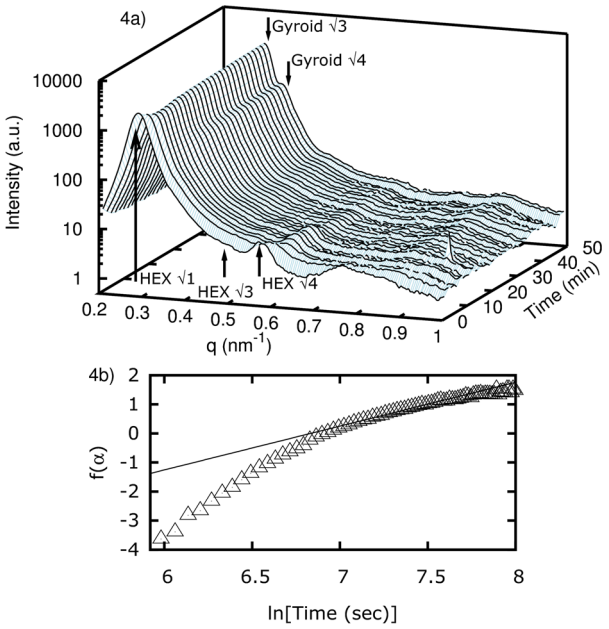

Figure 4. (a) Time evolution of the SAXS intensity $I(q)$ vs q following a 80−100 °C T-jump for 80% SI in DMP. (b) The fraction of transformed material expressed as $f(\alpha)$ vs $\ln[t]$ as described in the text shows the growth of the second-order peak of the gyroid. Time in this figure ranges from 6 to 50 min. The slope of the fitted line to the late-stage data gives the Avrami exponent n = 1.5.

that the two experiments probe different stages of the transformation. The Avrami analysis done on the T jumps focuses on the late-stage growth, whereas the FR equation is fit over the entire transition. The energy obtained from the FR analysis is the average of nucleation and growth energies, $(E_N + E_G)/2$, for the case m = 1, whereas the later stage probed in the T-jump may be dominated by the activation energy for growth, E_G. Thus, the larger activation energy obtained by T-ramp analysis suggests that $E_N > E_G$. These activation energies are similar in magnitude to those quoted by Floudas et al.,[14] 47−60 kcal/mol (200−250 kJ/mol) from SAXS and rheological kinetic experiments for HEX to gyroid transition in a PI−PEO melt.

In conclusion, we note that T-ramp data for different ramp rates (or different concentrations) can be collapsed to a single curve by shifting and scaling in terms of the temperature at which maximum growth occurs. The collapsed curve fits very well to the scaled univeral function derived by Farjas and Roura.[10,11] Using this method we were able to estimate the activation energy for the HEX → gyroid transition. We emphasize that this approach is of general applicability and encourage its use for analysis of nonisothermal kinetics measured in technically much easier to perform T-ramp experiments.

EXPERIMENTAL METHODS

SAXS experiments were carried out at beamline X10A of National Synchrotron Light Source (NSLS) at Brookhaven National Lab (BNL). Details of the experimental setup and data analysis are described in previous papers.[17,18] Briefly, the X-ray wavelength was 0.1089 nm (9.01 keV) with energy resolution of 1.1%. A two-dimensional (2D) CCD detector with an array of 1024 × 1024 was used to record the scattering pattern. 2D CCD images were azimuthally integrated to produce the scattering intensity profiles, $I(q)$, versus the magnitude of the scattering vector $q = (4\pi/\lambda)\sin\theta$ (2θ being the scattering angle), which were further processed in MATLAB, as described in previous works from our group.[17,18] The interval between successive frames of time-resolved SAXS measurements was 33 s (30 s data acquisition time + 3 s data transfer time). The SI diblock copolymer (Polymer Source, M_n = PS(16100)-*b*-PI(11200) [referred to as SI(16−11) in the text above], with M_w/M_n = 1.03) was dissolved in the solvent dimethyl phthalate (75%, 80% w/v) which is selective for the PS block. 2,6-Ditertibutyl-4-methyphenol (BHT), 0.5 wt %, was added to prevent polymer oxidization. Cyclohexane was added to the mixture as a cosolvent to dissolve the polymer solution. The solution was shaken until clear, following which the cyclohexane was removed by evaporation until there was no weight change in the sample over at least 24 h. Fitting was done using gnuplot's intrinsic fit command, which employs a nonlinear least-squares Marquardt−Levenberg algorithm.

ASSOCIATED CONTENT

Supporting Information

Figure S1. This material is available free of charge via the Internet at http://pubs.acs.org.

AUTHOR INFORMATION

Corresponding Author

*E-mail: rb@physics.bu.edu.

Notes

The authors declare no competing financial interest.

ACKNOWLEDGMENTS

We thank Dr. Steve Bennett for valuable assistance at x10A beamline of NSLS and acknowledge very helpful discussions with Drs. Milos Steinhart and Yongsheng Liu in designing and conducting the SAXS experiments. This research was supported by NSF Division of Materials Research award No. DMR 0804784. The SAXS measurements were carried out at NSLS of BNL, which is supported by the U.S. Department of Energy, Division of Materials Sciences and Division of Chemical Sciences under Contract No. DE-AC02-98CH10886.

REFERENCES

(1) Avrami, M. *J. Chem. Phys.* **1939**, *7*, 1103−1112.
(2) Avrami, M. *J. Chem. Phys.* **1940**, *8*, 212−224.
(3) Avrami, M. *J. Chem. Phys.* **1941**, *9*, 177−184.
(4) Johnson, W. A.; Mehl, R. F. *Trans. Am. Inst. Min. Metall. Eng.* **1939**, *135*, 416.
(5) Kolmogorov, A. N. *Bull. Acad. Sci. URSS* **1937**, *3*, 355−359.
(6) Ozawa, T. *Polymer* **1971**, *12*, 150.
(7) Kissinger, H. *Anal. Chem.* **1957**, *29*, 1702.
(8) Di Lorenzo, M. L.; Silvestre, C. *Prog. Polym. Sci.* **1999**, *24*, 917−950.
(9) Matusita, K.; Komatsu, T.; Ryosuke Yokota, R. *J. Mater. Sci.* **1984**, *19*, 291−296.
(10) Farjas, J.; Roura, P. *Acta Mater.* **2006**, *54*, 5573−5579.
(11) Farjas, J.; Roura, P. *J. Mater. Res.* **2008**, *23*, 418−426.
(12) Matsen, M. *Phys. Rev. Lett.* **1998**, *80*, 4470−4473.
(13) Cheng, X.; Lin, L.; Weinan, E.; Zhang, P.; Shi, A. *Phys. Rev. Lett.* **2010**, *104*, 148301.
(14) Floudas, G.; Ulrich, R.; Wiesner, U. *J. Chem. Phys.* **1999**, *110*, 652.
(15) Lodge, T. P.; Pudil, B.; Hanley, K. J. *Macromolecules* **2002**, *35*, 4707−4717.
(16) Wang, C.; Lodge, T. P. *Macromolecules* **2002**, *35*, 6997−7006.
(17) Liu, Y.; Li, M.; Steinhart, M.; Bansil, R. *Macromolecules* **2007**, *40*, 9482−9490.
(18) Li, M.; Liu, Y.; Nie, H.; Bansil, R. *Macromolecules* **2007**, *40*, 9491−9502.